

ac resistivity of d -wave ceramic superconductors

Mai Suan Li^{1,2} and Daniel Domínguez³

¹*Institute of Physics, Polish Academy of Sciences, Al. Lotnikow 32/46, 02-668 Warsaw, Poland*

²*Institut für Theoretische Physik, Universität zu Köln, Zùlpicher Straße 77, D-50937 Köln, Germany*

³*Centro Atómico Bariloche, 8400 S. C. de Bariloche, Rio Negro, Argentina*

(Received 5 April 2000)

We model d -wave ceramic superconductors with a three-dimensional lattice of randomly distributed π Josephson junctions with finite self-inductance. The linear and nonlinear ac resistivity of the d -wave ceramic superconductors is obtained as a function of temperature by solving the corresponding Langevin dynamical equations. We find that the linear ac resistivity remains finite at temperature T_p where the third harmonics of resistivity has a peak. The current amplitude dependence of the nonlinear resistivity at the peak position is found to be a power law. These results agree qualitatively with experiments. We also show that the peak of the nonlinear resistivity is related to the onset of the paramagnetic Meissner effect which occurs at the crossover temperature T_p , which is above the chiral glass transition temperature T_{cg} .

I. INTRODUCTION

The interplay of superconductivity and disorder in granular superconductors has been of great interest, particularly regarding their magnetic properties and glassy behavior.^{1,2} Granular superconductors are usually described as a random network of superconducting grains coupled by Josephson weak links.¹⁻⁴ In the last years, there has been a renewed interest in the study of this problem in high-temperature ceramic superconductors (HTCS's). Several experimental groups have found a paramagnetic Meissner effect (PME) at low magnetic fields.⁵ Sigrist and Rice⁶ proposed that this effect could be a consequence of the intrinsic unconventional pairing symmetry of the HTCS's of $d_{x^2-y^2}$ type.⁷ Depending on the relative orientation of the superconducting grains, it is possible to have weak links with negative Josephson coupling.^{6,7} These negative weak links, which are called π junctions, can give rise to the PME according to Refs. 5 and 6. In fact, a model d -wave granular superconductor, consisting of a network of Josephson junctions with a random concentration of π junctions and including magnetic screening, has been able to explain the paramagnetic Meissner effect observed at low fields.⁸ Also in this model, a phase transition to a *chiral glass* has been predicted for zero magnetic fields.⁹⁻¹² The frustration effect due to the random distribution of π junctions leads to a glass state of quenched-in "chiralities," which are local loop supercurrents circulating over grains and carrying a half-quantum of flux. Evidence of this transition has been related to measurements of the nonlinear ac magnetic susceptibility.¹³ Moreover, the random π -junction model has also been adequate to explain several dynamical phenomena observed in HTC's such as anomalous microwave absorption,¹⁴ the so-called compensation effect,¹⁵ and the effect of applied electric fields in the apparent critical current.¹⁶

In recent experiments Yamao *et al.*¹⁷ have measured the ac linear resistivity ρ_0 and the nonlinear resistivity ρ_2 of the ceramic superconductor $\text{YBa}_2\text{Cu}_4\text{O}_8$. Here ρ_0 and ρ_2 are defined as the first and third coefficients of the expansion of the voltage $V(t)$ in terms of the external current $I_{ext}(t)$:

$$V = \rho_0 I_{ext} + \rho_2 I_{ext}^3 + \dots \quad (1)$$

When the sample is driven by an ac current $I_{ext}(t) = I_0 \sin(\omega t)$, one can relate ρ_0 and ρ_2 to the first harmonics V'_ω and third harmonics $V'_{3\omega}$ in the following way:

$$\begin{aligned} \rho_0 &= V'_\omega / I_0, \\ \rho_2 &= -4V'_{3\omega} / I_0^3, \quad V'_{n\omega} = \frac{1}{2\pi} \int_{-\pi}^{\pi} V(t) \sin(n\omega t) d(\omega t), \\ n &= 1, 3. \end{aligned} \quad (2)$$

The key finding of Ref. 17 is that ρ_0 does not vanish even at and below the intergrain ordering temperature T_{c2} . On the other hand, ρ_2 has a peak near this temperature, which was found to be negative. In the chiral glass phase the $U(1)$ gauge symmetry is not broken and the phase of the condensate remains disordered.⁹⁻¹¹ The chiral glass phase, therefore, should not be superconducting but exhibit an Ohmic behavior with a finite resistance. Based on these theoretical predictions Yamao *et al.*¹⁷ speculated that their results give further support to the existence of the chiral glass phase, in addition to previous results from magnetic susceptibility measurements.¹³

Another interesting result of Yamao *et al.*¹⁷ is the power law dependence of $|V'_{3\omega}(T_p)/I_0^3|$ (or of ρ_2) at its maximum position T_p on I_0 : $|V'_{3\omega}(T_p)/I_0^3| \sim I_0^{-\alpha}$. The experimental value of the power law exponent was $\alpha \approx 1.1$.¹⁸

The goal of our paper is twofold. First, we try to reproduce the experimental results¹⁷ using the model of the Josephson junctions between d -wave superconducting grains^{8,9} where the screening of the external field by supercurrents is taken into account. Second, we discuss the question if the temperature T_p of the nonlinear resistivity peak and the transition temperature T_{cg} to the chiral glass phase^{10,11} are related. We calculate the linear and nonlinear ac resistivity by a Langevin dynamics simulation. In agreement with the experimental data¹⁷ we find that ρ_0 remains finite below and at the temperature T_p where ρ_2 has a peak. Furthermore, the

maximum value of $|V'_{3\omega}(T_p)/I_0^3|$ is found to scale with I_0 with a power law exponent $\alpha = 1.1 \pm 0.6$, which is close to the experimental value.¹⁷ However, we find that T_p is above the equilibrium chiral glass transition temperature T_{cg} .

II. MODEL

We neglect the charging effects of the grains and consider the following Hamiltonian:^{8,9}

$$\mathcal{H} = - \sum_{\langle ij \rangle} J_{ij} \cos(\theta_i - \theta_j - A_{ij}) + \frac{1}{2\mathcal{L}} \sum_p (\Phi_p - \Phi_p^{ext})^2, \quad (3)$$

$$\Phi_p = \frac{\phi_0}{2\pi} \sum_{\langle ij \rangle} A_{ij}, \quad A_{ij} = \frac{2\pi}{\phi_0} \int_i^j \vec{A}(\vec{r}) d\vec{r},$$

where θ_i is the phase of the condensate of the grain at the i th site of a simple cubic lattice, \vec{A} is the fluctuating gauge potential at each link of the lattice, ϕ_0 denotes the flux quantum, J_{ij} denotes the Josephson coupling between the i th and j th grains, and \mathcal{L} is the self-inductance of a loop (an elementary plaquette), while the mutual inductance between different loops is neglected. The first sum is taken over all nearest-neighbor pairs and the second sum is taken over all elementary plaquettes on the lattice. Fluctuating variables to be summed over are the phase variables θ_i at each site and the gauge variables A_{ij} at each link. Φ_p is the total magnetic flux threading through the p th plaquette, whereas Φ_p^{ext} is the flux due to an external magnetic applied along the z direction,

$$\Phi_p^{ext} = \begin{cases} HS & \text{if } p \text{ is on the } \langle xy \rangle \text{ plane,} \\ 0 & \text{otherwise,} \end{cases} \quad (4)$$

where S denotes the area of an elementary plaquette. For the d -wave superconductors we assume J_{ij} to be an independent random variable taking the values J or $-J$ with equal probability ($\pm J$ or bimodal distribution), each representing 0 and π junctions.

In order to study the dynamical response and transport properties, we model the current flowing between two grains with the resistively shunted junction (RSJ) model,^{3,4} which gives

$$I_{ij} = \frac{2e}{\hbar} J_{ij} \sin \theta_{ij} + \frac{\hbar}{2eR} \frac{d\theta_{ij}}{dt} + \eta_{ij}(t). \quad (5)$$

Here we add to the Josephson current the contribution of a dissipative Ohmic current due to an intergrain resistance R and the Langevin noise current $\eta_{ij}(t)$ which has correlations

$$\langle \eta_{ij}(t) \eta_{i'j'}(t') \rangle = \frac{2kT}{R} \delta_{i,i'} \delta_{j,j'} \delta(t-t'). \quad (6)$$

The dynamical variable in this case is the gauge invariant phase difference $\theta_{ij} = \theta_i - \theta_j - A_{ij}$. The total flux through each plaquette p depends on the mesh current C_p .

$$\Phi_p = \Phi_p^{ext} + \mathcal{L} C_p \quad (7)$$

The mesh currents C_p , the link currents I_{ij} , and the external current I_{ext} are related through current conservation. At this

point, it is better to redefine the notation: the site of each grain is at position $\mathbf{n} = (n_x, n_y, n_z)$ (i.e., $i \equiv \mathbf{n}$), the lattice directions are $\mu = \hat{\mathbf{x}}, \hat{\mathbf{y}}, \hat{\mathbf{z}}$, the link variables are between sites \mathbf{n} and $\mathbf{n} + \mu$ (i.e., link $ij \equiv$ link \mathbf{n}, μ), and the plaquettes p are defined by the site \mathbf{n} and the normal direction μ [i.e., plaquette $p \equiv$ plaquette \mathbf{n}, μ ; for example, the plaquette $\mathbf{n}, \hat{\mathbf{z}}$ is centered at position $\mathbf{n} + (\hat{\mathbf{x}} + \hat{\mathbf{y}})/2$]. The current $I_\mu(\mathbf{n})$ is related to the mesh currents $C_\nu(\mathbf{n})$ and the external current in the y direction as

$$I_\lambda(\mathbf{n}) = \varepsilon_{\lambda\mu\nu} \Delta_\mu^- C_\nu(\mathbf{n}) + \delta_{\lambda,y} I_{ext}, \quad (8)$$

where $\varepsilon_{\lambda\mu\nu}$ is the Levi-Civita tensor, Δ_μ^- is the backward difference operator, $\Delta_\mu^- C_\nu(\mathbf{n}) = C_\nu(\mathbf{n}) - C_\nu(\mathbf{n} - \mu)$, and repeated indices are summed. It is easy to verify that Eq. (8) satisfies current conservation. The magnetic flux $\Phi_\lambda(\mathbf{n})$ and the gauge invariant phases $\theta_\nu(\mathbf{n}) = \Delta_\nu^+ \theta(\mathbf{n}) - A_\nu(\mathbf{n})$ are related as

$$\Phi_\lambda(\mathbf{n}) = - \frac{\Phi_0}{2\pi} \varepsilon_{\lambda\mu\nu} \Delta_\mu^+ \theta_\nu(\mathbf{n}), \quad (9)$$

with the forward difference operator $\Delta_\mu^+ \theta_\nu(\mathbf{n}) = \theta_\nu(\mathbf{n} + \mu) - \theta_\nu(\mathbf{n})$.

Then, from Eqs. (5), (6), (8), and (9) we obtain the following dynamical equation:

$$\frac{\hbar}{2eR} \frac{d\theta_\mu(\mathbf{n})}{dt} = - \frac{2e}{\hbar} J_\mu(\mathbf{n}) \sin \theta_\mu(\mathbf{n}) - \delta_{\mu,y} I_{ext} - \frac{\hbar}{2e\mathcal{L}} \Delta_\nu^- [\Delta_\nu^+ \theta_\mu(\mathbf{n}) - \Delta_\mu^+ \theta_\nu(\mathbf{n})] - \eta_\mu(\mathbf{n}, t), \quad (10)$$

which represents the RSJ dynamics of a three-dimensional Josephson junction array with magnetic screening.^{4,8}

We can also obtain these equations from Eq. (3) if we add to \mathcal{H} the external current term: $\mathcal{H}_T = \mathcal{H} + \sum_{\mathbf{n}} (\hbar/2e) I_{ext} \theta_y(\mathbf{n})$. Then an equation of the Langevin form is obtained by taking derivatives with respect to the gauge invariant phase difference:

$$\frac{\hbar}{2eR} \frac{d\theta_\mu(\mathbf{n})}{dt} = - \frac{2e}{\hbar} \frac{\delta \mathcal{H}_T}{\delta \theta_\mu(\mathbf{n})} - \eta_\mu(\mathbf{n}, t), \quad (11)$$

leading to the RSJ dynamical equations of Eq. (10).¹⁹

In what follows we will consider currents normalized by $I_J = 2eJ/\hbar$, time by $\tau = \phi_0/2\pi I_J R$, voltages by RI_J , inductance by $\phi_0/2\pi I_J$, and temperature by J/k_B . We consider open boundary conditions for magnetic fields and currents in the same way as defined in Refs. 4 and 8.

III. RESULTS

The system of differential equations (10) is integrated numerically by a second order Runge-Kutta algorithm. We consider the system size $L=8$ and the self-inductance $\mathcal{L}=1$. Depending on values of I_0 and ω the number of samples used for the disorder averaging ranges between 15 and 40. The number of integration steps is chosen to be $10^5 - 5 \times 10^5$.

The temperature dependence of the linear resistivity ρ_0

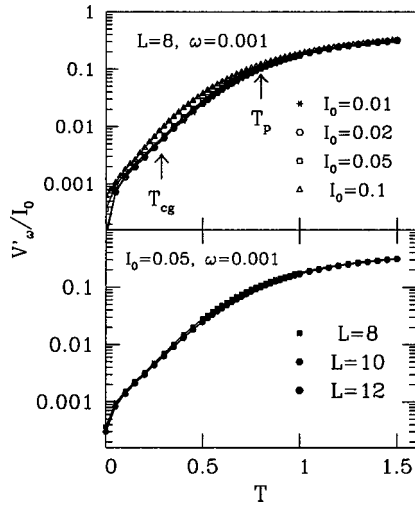


FIG. 1. (a) Upper panel: the temperature dependence of V'_ω/I_0 for $L=8$, $\mathcal{L}=1$ and $\omega=0.001$. The open triangles, squares, and hexagons correspond to $I_0=0.1, 0.05, 0.02$, and 0.01 . The arrows correspond to $T_p=0.8$ and $T_{cg}=0.286$, respectively. (b) Lower panel: the size dependence of V'_ω/I_0 for $I_0=0.05$, $\mathcal{L}=1$, and $\omega=0.001$. The number of time steps is equal to 10^5 . The results are averaged over 15–40 samples.

$=V'_\omega/I_0$ for different values of I_0 is shown in Fig. 1 (upper panel). At low temperatures we observe a weak dependence on I_0 , but for currents small enough ρ_0 becomes independent of current. From the lower panel of Fig. 1 it is clear that the V'_ω/I_0 becomes size independent for $L>10$. Thus, the linear resistivity is nonzero for all temperatures $T>0$ in the thermodynamic limit. This is in good agreement with the result that U(1) symmetry is not broken in the chiral glass state,^{9–11} and therefore there is no superconductivity for any finite T . We note that a similar result was obtained for the vortex glass state when the magnetic screening is taken into account.²⁰

In Fig. 2 we analyze the nonlinear resistivity $\rho_2 = -4V'_{3\omega}(T)/I_0^3$. We find that it has a negative maximum at a temperature T_p . This characteristic maximum depends on I_0 , but we can fit its position in temperature at $T_p=0.8 \pm 0.05$ for all values of I_0 presented in Fig. 2. The arrow in Fig. 1 also indicates the position of the temperature T_p . We see that for $T \gg T_p$ the linear resistivity ρ_0 is independent of current for a large range of currents I_0 . On the other hand,

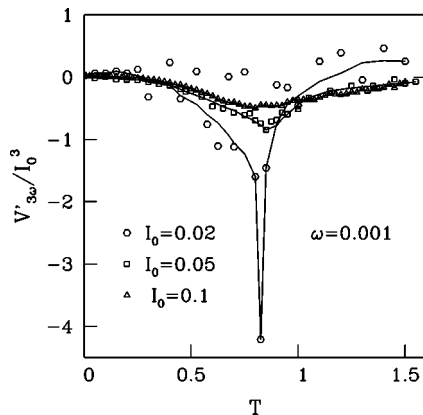


FIG. 2. The same as in Fig. 1 but for $|V'_{3\omega}(T_p)/I_0^3|$.

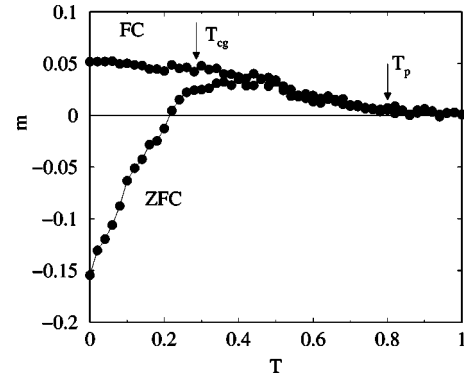


FIG. 3. The temperature dependence of the magnetization m in FC and ZFC regimes for the d -wave superconductors. $L=8$ and $\mathcal{L}=1$. The results are averaged over 25 samples.

below T_p the resistivity ρ_0 is current dependent for an intermediate range of I_0 and only for very low currents ρ_0 becomes current independent.

We identify T_p to correspond to the intergrain ordering transition temperature above which the thermoremanent magnetization disappears in the experiment of Ref.17. In order to verify this, we study in Fig. 3 the magnetization at a finite magnetic field $f=HS/\phi_0=0.1$. We show both the zero-field cooling (ZFC) and field cooling (FC) curves.⁸ We can see that T_p is the temperature where there is an onset of positive magnetization, i.e., the paramagnetic Meissner effect, starts to be observed. On the other hand, the irreversibility point occurs at temperatures lower than T_p , and its position is dependent on the heating or cooling rate. It should also be noted that above T_p the real part of the linear magnetic susceptibility vanishes (see Fig. 18 from Ref. 9).

The results presented in Figs. 1, 2, and 3 are in good agreement with the experimental data.¹⁷ From this point of view our findings and the experimental results¹⁷ may seem compatible with the chiral glass picture.¹¹ However, T_p is remarkably higher than the chiral glass temperature T_{cg} obtained previously (for $\mathcal{L}=1$, $T_{cg}=0.286$, see Ref. 10). Then we conclude that the peak of ρ_2 has no relation to the chiral glass phase transition. Thus, T_p just separates the normal-state phase from a “chiral paramagnet” where there are local chiral magnetic moments. These local moments can be polarized under an external magnetic field, and therefore one can observe the paramagnetic Meissner effect under a low external field below T_p . At a lower temperature, collective phenomena due to the interactions among the chiral moments will start to be important, leading to the transition to the chiral glass state. This last transition should show in the nonlinear chiral glass susceptibility which should diverge at T_{cg} .^{10,11} The chiral glass transition may also be reflected in the irreversibility point in the FC and ZFC magnetizations. Although our model is different from the corresponding gauge glass model,²⁰ one can expect that here the screening spoils any glassy phase except the chiral glass. The linear resistivity is, therefore, nonzero for finite temperatures.

Our calculation of the nonlinear ac resistivity ρ_2 is a non-equilibrium calculation at a finite frequency ω and finite ac current amplitude I_0 . Therefore, one should be concerned about the finite- ω and finite- I_0 effects. In particular, one may ask if it is possible that the temperature T_p of the peak in ρ_2

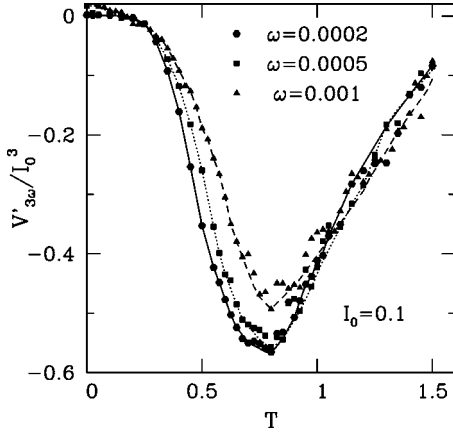


FIG. 4. The temperature dependence of $V'_{3\omega}(T)/I_0^3$. The solid triangles, squares, and hexagons correspond to $\omega=0.001, 0.0005$, and 0.0002 , respectively. $L=8$, $\mathcal{L}=1$, and $I_0=0.1$. The results are averaged over 15 samples.

will tend to T_{cg} in the limit $\omega \rightarrow 0$, $I_0 \rightarrow 0$. We have carefully studied this possibility. Figure 4 shows the temperature dependence of ρ_2 for various values of ω and $I_0=0.1$. From Figs. 2 and 4 it is clear that the position of T_p depends on I_0 and ω very weakly. It is, therefore, unlikely that T_p tends to T_{cg} as $\omega \rightarrow 0$ and $I_0 \rightarrow 0$.

In accordance with the experiments of Yamao *et al.*,¹⁷ the negative maximum of $V'_{3\omega}(T_p)/I_0^3$ shows up. Furthermore, the height of peaks of $|V'_{3\omega}(T_p)/I_0^3|$ increases with the decrease of ω and saturates at small frequencies (see Fig. 4). Such a tendency was also observed experimentally.¹⁷

In order to get more insight into the nature of T_p we have calculated the specific heat C_v , which is defined as proportional to the energy fluctuations, $C_v = \langle (\delta E)^2 \rangle / k_B T^2$. The results are shown in Fig. 5. There is a broad peak in C_v located at T_p and well above T_{cg} . Similar to the spin glass case where the peak of specific heat is positioned higher than the critical temperature to the glass phase,²¹ we conclude that T_p does not correspond to a phase transition to a long-range-ordered phase.

A more convincing conclusion about the nature of the peak in the nonlinear susceptibility should be obtained from

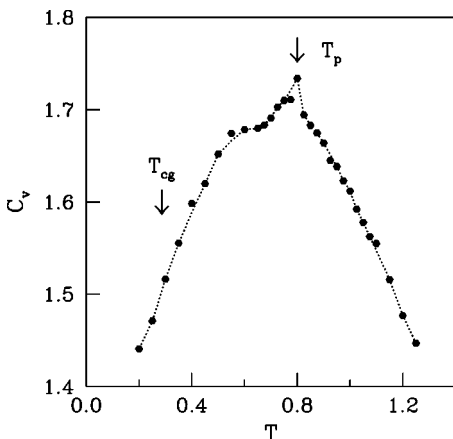


FIG. 5. The temperature dependence of C_v obtained by Monte Carlo simulations for $L=8$ and $\mathcal{L}=1$. The results are averaged over 20 samples. The error bars are smaller than the symbol sizes.

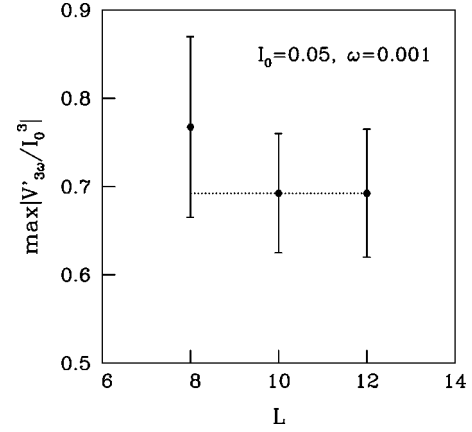


FIG. 6. The dependence of the maximal values of $|V'_{3\omega}(T_p)/I_0^3|$ on the system size L . $I_0=0.05$, $\mathcal{L}=1$, and $\omega=0.001$. The results are averaged over 15–40 samples.

a finite-size analysis. Figure 6 shows the dependence of $\max|V'_{3\omega}/I_0^3|$ on the system size L for $I_0=0.05$ and $\omega=0.001$. Clearly, the height of the peak does not diverge as $L \rightarrow \infty$. In other words, the peak in the nonlinear resistivity does not correspond to a phase transition in the thermodynamic limit.

Figure 7 shows the log-log plot for the dependence of the maximal values of $|V'_{3\omega}(T_p)/I_0^3|$ on I_0 for a fixed frequency $\omega=0.001$. One can fit $\max|V'_{3\omega}(T_p)/I_0^3| \sim I_0^\alpha$ with $\alpha=1.1 \pm 0.6$, giving more weight to small values of I_0 . So within the error bars our estimate of α agrees with that obtained by the experiments.^{17,18}

IV. DISCUSSION

In Ref. 17 it was argued that the peak of the nonlinear resistivity was a signal of the transition to the chiral glass state. The value of T_p obtained in our simulations is, however, considerably higher than the chiral glass transition temperature T_{cg} . We conclude that the peak of ρ_2 is not related to the transition to the chiral glass. T_p is found to coincide with the point for the onset of the paramagnetic Meissner

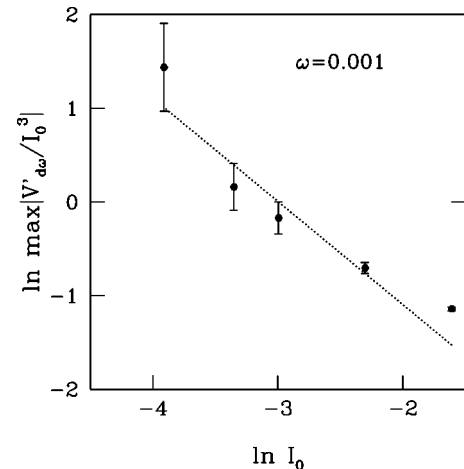


FIG. 7. The dependence of the maximal values of $|V'_{3\omega}(T_p)/I_0^3|$ on I_0 . Here $L=8$, $\mathcal{L}=1$, and $\omega=0.001$. The results are averaged over 15–40 samples.

effect, where the magnetization becomes positive. In this respect, our result agrees with the experimental result.¹⁷ We interpret T_p as the crossover temperature from the normal-state phase to a “chiral paramagnet” in which there are local chiral magnetic moments induced by the π junctions. As the temperature is lowered the system would have a phase transition from the chiral paramagnetic phase to the chiral glass state. At this critical point ρ_2 does not show any particular feature. Furthermore, we found that the linear resistivity is always finite at $T > 0$ due to screening effects, and therefore there is no superconductivity in the random π -junction model.

In conclusion, the experimental results of Yamao *et al.*¹⁷ can be reproduced by the XY -like model for d -wave super-

conductors. Contrary to the speculation of Ref. 17 we expect that T_p does not correspond to the chiral glass transition.

ACKNOWLEDGMENTS

One of us (M.S.L.) thanks M. Cieplak, H. Kawamura, A. Majhofer, T. Nattermann, and M. Sigríst for useful discussions. Financial support from the Polish agency KBN (Grant No. 2P03B-146-18) is acknowledged. D.D. acknowledges financial support from Fundación Antorchas (Proy. A-13532/1-96), ANPCyT (PICT-03-00121-02151), and Conicet and CNEA (Argentina). We also acknowledge financial support from the International Centre for Theoretical Physics.

-
- ¹C. Ebner and D. Stroud, Phys. Rev. B **31**, 165 (1985).
²J. Choi and J. V. José, Phys. Rev. Lett. **62**, 320 (1989).
³J. S. Chung, K. H. Lee, and D. Stroud, Phys. Rev. B **40**, 6570 (1989); F. Falo, A. R. Bishop, and P. S. Lomdalhl, *ibid.* **41**, 10 983 (1990); Y. H. Li and S. Teitel, Phys. Rev. Lett. **65**, 2595 (1990); M. S. Rzchowski, S. P. Benz, M. Tinkhem, and C. J. Lobb, Phys. Rev. B **42**, 2041 (1990); K. H. Lee and D. Stroud, *ibid.* **44**, 9780 (1991); D. Reinell, W. Dieterich, T. Wolf, and A. Majhofer, *ibid.* **49**, 9118 (1994); M. Capezzali, H. Beck, and S. R. Shenoy, Phys. Rev. Lett. **78**, 523 (1997).
⁴D. Domínguez and J. V. José, Phys. Rev. B **53**, 11 692 (1996).
⁵P. Svelindh, K. Niskanen, P. Nordblad, L. Lundgren, B. Lönnberg, and T. Lundström, Physica C **162-164**, 1365 (1989); W. Braunisch, N. Knauf, V. Kataev, S. Neuhausen, A. Grutz, A. Kock, B. Roden, D. Khomskii, and D. Wohlleben, Phys. Rev. Lett. **68**, 1908 (1992); Phys. Rev. B **48**, 4030 (1993); Ch. Heinzl, Th. Theilig, and P. Ziemann, *ibid.* **48**, 3445 (1993); S. Riedling, G. Bräuchle, R. Lucht, K. Röhberg, and H. v. Löhneysen, *ibid.* **49**, 13 283 (1994); J. Kötzler, M. Baumann, and N. Knauf, *ibid.* **52**, 1215 (1995); E. I. Papadopoulou, P. Nordblad, X. Svendlindh, S. Schöneberger, and R. Gross, Phys. Rev. Lett. **82**, 173 (1999).
⁶M. Sigríst and T. M. Rice, J. Phys. Soc. Jpn. **61**, 4283 (1992).
⁷D. A. Wollman *et al.*, Phys. Rev. Lett. **74**, 797 (1994); D. J. van Harlingen, Rev. Mod. Phys. **67**, 515 (1995).
⁸D. Domínguez, E. A. Jagla, and C. A. Balseiro, Phys. Rev. Lett. **72**, 2773 (1994).
⁹H. Kawamura and M. S. Li, Phys. Rev. B **54**, 619 (1996).
¹⁰H. Kawamura and M. S. Li, Phys. Rev. Lett. **78**, 1556 (1997).
¹¹H. Kawamura and M. S. Li, J. Phys. Soc. Jpn. **66**, 2110 (1997).
¹²H. Kawamura, J. Phys. Soc. Jpn., Suppl. **69**, 281 (2000).
¹³M. Matsuura, M. Kawacki, K. Miyoshi, M. Hagiwara, and K. Koyama, J. Phys. Soc. Jpn. **64**, 4540 (1995).
¹⁴D. Domínguez, E. A. Jagla, and C. A. Balseiro, Physica (Amsterdam) **235C-240C**, 3283 (1994).
¹⁵M. S. Li, Phys. Rev. B **60**, 118 (1999).
¹⁶D. Domínguez, C. Wiecko, and J. V. José, Phys. Rev. Lett. **83**, 4164 (1999).
¹⁷T. Yamao, M. Hagiwara, K. Koyama, and M. Matsuura, J. Phys. Soc. Jpn. **68**, 871 (1999).
¹⁸We have extracted the experimental value of $\alpha \approx 1.1$ from Fig. 7 of Ref. 17.
¹⁹If the derivatives in Eq. (11) are taken with respect to the local phase $\theta(\mathbf{n})$ instead of $\theta_\mu(\mathbf{n})$, the so-called time-dependent Ginzburg-Landau (TDGL) dynamics is obtained. In the TDGL case there is on-site dissipation and current is not conserved.
²⁰H. S. Bokil and A. P. Young, Phys. Rev. Lett. **74**, 3021 (1995).
²¹K. Binder and P. A. Young, Rev. Mod. Phys. **58**, 801 (1986).